Mausam, (1990), **41**, 2, 241-250

551.513.1 : 551.557.5

Barotropic spectral modelling of non-linear interaction for transient waves in tropical easterly jet

S. K. MISHRA

Indian Institute of Tropical Meteorology, Pune

सार - 100 मि. बार पर माध्य मानसून उष्णकटिबंधीय पूर्वी जेट के आरम्भिक सकल रैखिक दाब घनत्वी अस्थिर प्रणाली के लिए गोलक पर तरंग-क्षेत्र प्रवाह और तरंग-तरंग अन्योन्य क्रियाओं का अध्ययन किया गया। इस अध्ययन के लिए 120 दिनों के लिए रुंडन (छेदन) $N=20$ और $M=40$ के साथ अनपसारी दाब घनत्वी गोलाकार मानावली निदर्श का समाकलन किया गया। इसमें देखा गया कि तरंग क्षेत्र प्रवाह अन्योन्य क्रिया तरंग गतिक ऊर्जा और इनस्ट्राफी में 35-दिन की अवधि के साथ दोलन की ओर ले जाती है। क्षेत्रीय कोणीय संवेग वाहन और तरंग के वृद्धि क्षय चक्र के मध्य संबंध की खोज की गई है। तरंग-तरंग अन्योन्य क्रिया 25-35 दिनों के मध्य निम्न आवृति दोलन की अवधि में भिन्नता लाने के लिए उत्तरदायी है। माध्य गतिक ऊर्जा और इनस्ट्राफी मानावली और तरंग संख्या प्रांत में तरंग-तरंग अन्योन्य क्रिया का समाकलन किया गया और तरंगों के अरैखिक मूल्यांकन में उनकी भूमिका पर विचार विमर्श किया गया है।

ABSTRACT. The wave-zonal flow and wave-wave interactions are studied over the sphere for the initial single linear barotropic unstable mode of the mean monsoon tropical easterly jet at 100 mb. The non-divergent barotropic global spectral model with truncation $N=20$ and $M=40$ is integrated for 120 days for the study. It is found that the wave-zonal flow interaction leads to an oscillation with a period of 35 days in the wave kinetic energy and enstrophy. The relation between the zonal angular momentum transport and growth-decay cycle of the wave is explored. The wave-wave interaction is responsible for the variation in the period of low frequency oscillation between 25&35 days. The mean kinetic energy and enstrophy spectra, and wave-wave interaction in the wave number domain are computed and their role in the non-linear evolution of the waves is discussed.

1. Introduction

The linear dynamics of inviscid barotropic and barotropic-baroclinic unstable waves associated with the observed zonal flow of tropical easterly jet have been studied by using dry quasi-geostrophic β-plane models (Mishra *et al.* 1981, Mishra and Tandon 1983). Mishra (1987) has investigated the effects of spherical geometry on the linear dynamics of the barotropic unstable wave. Tupaz *et al.* (1978) considered an easterly Bickley jet that has slow zonal variation and studied the down stream amplification of westward propagating, barotropic, Rossby wave disturbance. Schoeberl and Lindzen (1984) have performed numerical integration by using non-divergent barotropic vorticity equation in order to understand the evolution of the point easterly jet instability as it interacts with the mean flow in presence of single and multiple waves. They also found that the role of wave-wave interaction in the evolution process is unimportant.

Kwon and Mak (1988) extensively studied the non-linear equilibration process in a forced, dissipative barotropic β-plane model. They prescribed external forcing in the form of an easterly Bickley jet. They found that the equilibrium state may be either a steady wave state, a vacillation cycle or a chaos depending upon the values of two non-dimensional damping and forcing paramenters. The effect of non-linear processes was found relatively minor in the down stream amplification of westward propagating Rossby wave in a barotropic easterly jet having inhomogeneous horizontal shear (William *et al.* 1984).

In this study, it is proposed to investigate the influence of single wave-flow interaction and wave-wave interaction in the evolution of barotropic instability of the observed tropical easterly jet. Further, the experiment is performed by using barotropic model over the sphere.

2. Model and energetics

(a) *Quasi-linear model*

In quasi-linear motions, the wave-zonal flow interaction is allowed while the wave-wave interaction is suppressed. The quasi-linear motion is governed by a linear perturbation equation and a zonal mean equation. The author has studied the linear dynamics of barotropic unstable wave over the spherical earth by using the linear barotropic vorticity equation (Mishra 1987; hereafter referred to as M87). The barotropic quasi-linear motion over the sphere is governed by the following system of equations :

$$\frac{\partial q'}{\partial t} + \frac{\overline{U}}{a(1-\mu^2)}\frac{\partial q'}{\partial \lambda} + \frac{V'}{a}\frac{\partial \overline{q}}{\partial \mu} = 0 \qquad 1(a)$$

$$\frac{\partial \bar{q}}{\partial t} + \frac{1}{a} \frac{\partial (\overline{V'q'})}{\partial \mu} = 0 \qquad 1(b)$$

where,

$$q' = \nabla^2 \Psi' - R_e^{-2} \Psi'$$

$$\bar{q} = \nabla^2 \bar{\Psi} + 2\Omega\mu - R_e^{-2} \bar{\Psi}$$

$$\bar{U} = \bar{u} \cos \phi$$

$$V' = v' \cos \phi$$

$$\mu = \sin \phi$$

In the above equations the over bar and prime denote the basic state (zonal average) and perturbation quantities respectively. q is the potential vorticity and Ψ is the streamfunction. a is the radius of earth, ϕ and λ are the latitude and longitude respectively, R_e is the equatorial Rossby radius of deformation, whose value is 1900 km as computed in M87. The term involving R_e describes the free surface effect contribution to the potential vorticity.

Vorticity generation by source term and its dissipation by frictional processes are not included in Eqns. 1 [(a) & (b)]. It may be noted that the linear vorticity equation [Eqn. 1 (a)] allows the nonlinear interactions between different meridional modes.

(b) *Kinetic energy and enstrophy equations for quasi-linear model*

For clearer diagnostic of wave-mean flow interaction processes, the enstrophy, equation in addition to the kinetic energy equation, is used in this study. It may be recalled here that the barotropic instability criterion is given only in terms of the potential vorticity of the basic flow. The global average kinetic energy equation is obtained by multiplying Eqn. 1 (a) by $-\Psi'$ and averaging over the sphere. After some simple manipulations, the equation can be written as :

$$\frac{\partial}{\partial t} \tfrac{1}{2} \langle \overline{\nabla \Psi' . \nabla \Psi'} \rangle = \left\langle - \frac{\bar{U}}{a(1-\mu^2)} \frac{\partial (\overline{U'V'})}{\partial \mu} \right\rangle - R_e^{-2} \frac{\partial \langle \overline{\Psi' v'} \rangle}{\partial t} \qquad (2)$$

where the symbol $\langle\ \rangle$ denotes meridional average. $\langle\ \rangle = \frac{1}{2} \int_{-1}^{1} (\ ) d\mu$. The left hand side term of Eqn. (2) denotes the time tendency of the global average kinetic energy: the first term on the right hand side denotes the barotropic conversion of basic state kinetic energy into the wave kinetic energy and the last term stands for time tendency of the wave potential energy associated with the free surface. $\overline{U'V'}$ denotes the wave meridional flux of zonal angular momentum.

The global average enstrophy equation is obtained by multiplying Eqn. 1 (a) by q' and taking average over the sphere. The enstrophy equations is finally written as :

$$\frac{\partial \tfrac{1}{2} \langle \overline{q'^2} \rangle}{\partial t} = \frac{1}{a} \left\langle q \frac{\partial (\overline{V'q'})}{\partial \mu} \right\rangle \qquad (3)$$

where $\frac{1}{2} \overline{q'^2}$ denotes the wave enstrophy. The left hand side of Eqn. (3) represents the time tendency of the global average enstrophy and the right hand side term represents the conversion from basic state enstrophy $\langle \frac{1}{2} \bar{q}^2 \rangle$ to the wave enstrophy $\langle \frac{1}{2} \overline{q'^2} \rangle$. $\overline{V'q'}$ denotes the meridional flux of wave enstrophy.

The right hand side term of Eqn. (3) can be expressed after integrating by parts and using the fact that $\overline{V'q'} = 0$ at $\mu = \pm 1$, as $-\frac{1}{a} \left\langle \overline{V'q'} \frac{\partial \bar{q}}{\partial \mu} \right\rangle$.

Thus the wave enstrophy increases, or the conversion of potential vorticity from basic flow to the wave takes place when the wave potential vorticity flux is down-gradient of the basic state potential vorticity. In case of unstable wave the flux is northward in the region of negative $\frac{\partial \bar{q}}{\partial \mu}$. For non-divergent motion, the following relationship between momentum transport and potential vorticity transport is easily obtained:

$$\overline{V'q'} = -\frac{1}{a} \frac{\partial (\overline{U'V'})}{\partial \mu} \qquad (4)$$

It can be easily shown from Eqn. (4) and using the condition $\overline{U'V'} = 0$ at $\mu = \pm 1$ that :

$$\langle \overline{V'q'} \rangle = 0 \qquad (5)$$

This implies that the global average wave potential vorticity transport vanishes.

(c) *Non-linear model*

The evolution of two-dimensional non-divergent motions under non-linear interactions is governed by the following barotropic vorticity equation :

$$\frac{\partial q}{\partial t} + \frac{1}{a(1-\mu^2)} \frac{\partial}{\partial \lambda} (Uq) + \frac{1}{a} \frac{\partial}{\partial \mu} (Vq) = 0 \qquad (6)$$

where $q = \nabla^2 \Psi + 2\Omega\mu - R_e^{-2} \Psi$ is the total potential vorticity and $q = \bar{q} + q'$. In the equation, the non-linear interaction is due to the advection of potential vorticity as denoted by the last two terms of the equation. Eqn. (6) conserves the energy and enstrophy.

(d) *Numerical method*

The initial state as a single zonal wave superimposed on a zonal flow is only considered in this study. The non-linear interactions lead to subsequent generation of waves with zonal wavenumbers which are integer multiple of the zonal wavenumber of the given initial wave. The spectral method is used to find the solution of Eqn. (6). For this purpose, the stream function is expanded as a truncated spherical harmonic series :

$$\Psi(\lambda, \phi, t) = \sum_{m=0,s}^{M} \sum_{n=m}^{m+N} \left(\Psi^{m}_{1,n} \cos m\lambda + \Psi^{m}_{2,n} \sin m\lambda \right) P^{m}_{n}(\mu) \qquad (7)$$

where $P_n^m(\mu)$ is the associated Legendre function normalised to unity over the sphere, m is the zonal wavenumber, $n-m+1$ is the pseudo-latitudinal wavenumber, n is the two-dimensional wavenumber and $\psi^m_{1,n}$ $\psi^m_{2,n}$ are the spectral (spherical harmonic) coefficients of the streamfunction. M and N are the orders of truncation of the series in m and n respectively. The first summation goes from 0 to M at the interval of s. The half-transform method is used to evaluate the non-linear terms. The spectral coefficients are given by :

$$\Psi^m_{1,n} = \frac{1}{\pi}\int_0^{2\pi}\int_{-1}^{1}\Psi\, P_n^m \cos m\lambda\, d\mu\, d\lambda$$

$$\Psi^m_{2,n} = \frac{1}{\pi}\int_0^{2\pi}\int_{-1}^{1}\Psi\, P_n^m \sin m\lambda\, d\mu\, d\lambda$$

for $m \geqslant s$

$$\Psi^0_{1,n} = \frac{1}{2\pi}\int_0^{2\pi}\int_{-1}^{1}\Psi\, P_n^0\, d\mu\, d\lambda \text{ for } m = 0 \qquad (8)$$

The Euler-backward and leap-frog time differencing schemes are used for the first and for subsequent time steps, respectively. Robert's time filter with the filter parameter of .01 is used for damping temporal oscillation.

In the single wave-zonal flow interaction experiments, for intital wave number s, the spectral equations for $m=0$ and s are only integrated. The spectral equations for $m = 0,\ s,\ 2s, \ldots\ldots$ Integer (M/s) are integrated in non-linear experiment for initial single waves.

(e) *Spectral kinetic energy and enstrophy equations for non-linear model*

A better understanding of non-linear interaction particularly wave-wave interaction processes can be achieved by use of kinetic energy and enstrophy equations in the zonal (m) and two-dimensional (n) wavenumber domain. Kinetic energy per unit mass (k) for non-divergent horizontal motion can be written as:

$$k = \tfrac{1}{2}\nabla\Psi.\nabla\Psi = \tfrac{1}{2}\nabla.(\Psi\nabla\Psi) - \tfrac{1}{2}\Psi\nabla^2\Psi \qquad (9)$$

The global average kinetic energy (K) is obtained from Eqn. (9) in the following form :

$$K = \frac{1}{4\pi}\int_0^{2\pi}\int_{-1}^{1} k\, d\mu\, d\lambda$$

$$= \frac{1}{8\pi}\int_0^{2\pi}\int_{-1}^{1} -\Psi\nabla^2\Psi\, d\mu\, d\lambda \qquad (10)$$

Following relation is noted:

$$\nabla^2\Psi = \sum_{m=0,s}^{M}\sum_{n=m}^{m+N}\frac{-n(n+1)}{a^2}\left(\Psi^m_{1,n}\cos m\lambda + \Psi^m_{2,n}\sin m\lambda\right) P_n^m(\mu) \qquad (11)$$

On substituting the truncated series expansions (7) and (11) into Eqn. (10) and using orthogonality condition for the spherical harmonics, we get :

$$K = \frac{1}{4a^2}\sum_{n=0}^{N} n(n+1)\,\Psi^m_{1,n}\,\Psi^m_{1,n} + \frac{1}{8a^2}\sum_{m=s}^{M}\sum_{n=s}^{s+N} n(n+1)\left(\Psi^m_{1,n}\,\Psi^m_{1,n} + \Psi^m_{2,n}\,\Psi^m_{2,n}\right) \qquad (12)$$

Let K_n^m denote the global average kinetic energy of the (m, n) mode of the motion. Then we can write

$$K = \sum_{m=0,s}^{M}\sum_{n=m}^{m+N} K_n^m \qquad 12(a)$$

where,

$$K_n^m = \frac{n(n+1)}{8a^2}\left(\Psi^m_{1,n}\,\Psi^m_{1,n} + \Psi^m_{2,n}\,\Psi^m_{2,n}\right), \text{ for } m \geqslant s$$

and

$$K_n^0 = \frac{n(n+1)}{4a^2}\,\Psi^0_{1,n}\,\Psi^0_{1,n}, \text{ for } m = 0 \qquad 12(b)$$

To obtain the kinetic energy equation in terms of wavenumber, Eqn. 12(a) is differentiated with respect to time :

$$\frac{\partial}{\partial t}K_n^m = \frac{n(n+1)}{4a^2}\left(\Psi^m_{1,n}\frac{\partial\Psi^m_{1,n}}{\partial t} + \Psi^m_{2,n}\frac{\partial\Psi^m_{2,n}}{\partial t}\right) \qquad 13(a)$$

$$\frac{\partial K_n^0}{\partial t} = \frac{n(n+1)}{2a^2}\,\Psi^0_{1,n}\frac{\partial\Psi^0_{1,n}}{\partial t} \qquad 13(b)$$

The above equation contains the tendency of spherical harmonic coefficients of the stream function, which can be obtained by a spectral transformation of the vorticity equation [Eqn. (6)]. Finally, the kinetic energy equation in the m, n wavenumber domain can be written in the form :

$$\frac{\partial}{\partial t}K_n^m = \frac{1}{4}\left(\Psi^m_{1,n}\,J^m_{1,n} + \Psi^m_{2,n}\,J^m_{2,n}\right) - \frac{R_e^{-2}}{4a^2}\frac{\partial}{\partial t}\left(\Psi^m_{1,n}\,\Psi^m_{1,n} + \Psi^m_{2,n}\,\Psi^m_{2,n}\right)$$

for $m \geqslant s$ 14(a)

$$\frac{\partial}{\partial t}K_n^0 = \frac{1}{2}\left(\Psi^0_{1,n}\,J^0_{1,n}\right) - \frac{R_e^{-2}}{2a^2}\frac{\partial}{\partial t}\left(\Psi^0_{1,n}\,\Psi^0_{1,n}\right) \qquad 14(b)$$

where the first term of R.H.S. of Eqn. 14(a) represents the gain of kinetic energy by the m, n mode due to non-linear (wave-zonal flow + wave-wave) interactions. $J^m_{1,n}$ and $J^m_{2,n}$ are the spherical harmonic coefficients of the advection term of the vorticity equation :

$$J = \frac{1}{a(1-\mu^2)} \frac{\partial}{\partial \lambda} (U \nabla^2 \Psi) + \frac{1}{a} \frac{\partial}{\partial \mu} (V \nabla^2 \Psi) \qquad (15)$$

The kinetic energy equation in the zonal wavenumber domain can be easily obtained by summing Eqns. 14(a) and 14(b) over the order n :

$$\frac{\partial}{\partial t} K_m = \frac{\partial}{\partial t} \sum_{n=m}^{m+N} K^m_n = \frac{1}{4} \sum_{n=m}^{m+N} \left(\Psi^m_{1,n} J^m_{1,n} + \Psi^m_{2,n} J^m_{2,n} \right) - \frac{R_e^{-2}}{4a^2} \frac{\partial}{\partial t} \sum_{n=m}^{m+N} \left(\Psi^m_{1,n} \Psi^m_{1,n} + \Psi^m_{2,n} \Psi^m_{2,n} \right),$$

for $m \geq s$ 16(a)

$$\frac{\partial K_0}{\partial t} = \frac{1}{2} \sum_{n=1}^{N} \Psi^0_{1,n} J^0_{1,n} - \frac{R_e^{-2}}{2a^2} \frac{\partial}{\partial t} \sum_{n=1}^{N} \Psi^0_{1,n} \Psi^0_{1,n} \qquad 16(b)$$

The first term on the right hand side of Eqn. 16(a) represents the kinetic energy gain of wave m due to the wave-wave interactions and its interaction with the zonal flow. It may be recalled that the first term on right of Eqn. (2) gives the kinetic energy gain of wave m due to the wave-zonal flow interaction, which can be written in the spectral form as :

$$C(K_0, K_m) = \frac{1}{4a} \int_{-1}^{1} \sum_{n=0}^{N} U^0_{1,n} \frac{P^0_n}{(1-\mu^2)} \left(U_{1,m} V_{1,m} + U_{2,m} V_{2,m} \right) \mu \, d\mu \qquad 16(c)$$

where, $\frac{1}{2}(U_{1,m}V_{1,m} + U_{2,m}V_{2,m})$ is the zonal average momentum transport at a latitude due to wavenumber m. The integral in Eqn. 16 (c) is evaluated by using Gaussian quadrature method. The net gain of K.E. at the wavenumber m due to its interaction with all other waves (wave-wave interaction) is obtained as the difference between the first term on the right of Eqns. 16(a) and 16(c). When Eqn. (14) is summed over the zonal wavenumber m, the resulting equation is the kinetic energy equation in the two-dimensional wave number n domain :

$$\frac{\partial}{\partial t} K_n = \frac{1}{2} (\Psi^0_{1,n} J^0_{1,n}) + \frac{1}{4} \sum_{m=s,s}^{n} \left(\Psi^m_{1,n} J^m_{1,n} + \Psi^m_{2,n} J^m_{2,n} \right) - \frac{R_e^{-2}}{2a^2} \frac{\partial}{\partial t} (\Psi^0_{1,n} \Psi^0_{1,n}) - \frac{R_e^{-2}}{4a^2} \frac{\partial}{\partial t} \sum_{m=s,s}^{n} \left(\Psi^m_{1,n} \Psi^m_{1,n} + \Psi^m_{2,n} \Psi^m_{2,n} \right) \qquad (17)$$

The first two terms on the right of Eqn. (17) denote the gain of K.E. at the wavenumber n due to its interaction with all other wave numbers including zonal flow. It is not possible in this case to separate out the wave-wave interaction as has been achieved in the case of zonal wavenumber m. Further, the sum of non-linear interaction term over the wavenumber n should vanish in order to conserve the energy.

Let E_N is the global average enstrophy per unit mass, which can be written as :

$$E_N = \frac{1}{4\pi} \int_0^{2\pi} \int_{-1}^{1} \tfrac{1}{2} q^2 \, d\mu \, d\lambda \qquad 18(a)$$

It can be easily shown that :

$$E_N = \sum_{m=0,s}^{M} \sum_{n=m}^{m+N} (E_N)^m_n \qquad 18(b)$$

where $(E_N)^m_n$ is the enstrophy of (m, n) mode, which can be expressed as :

$$(E_N)^m_n = \frac{1}{8} (q^m_{1,n} q^m_{1,n} + q^m_{2,n} q^m_{2,n})$$

for $m \geq s$ 19(a)

$$(E_N)^0_n = \frac{1}{4} q^0_{1,n} q^0_{1,n} \quad \text{for } m = 0 \qquad 19(b)$$

where $q^m_{1,n}$, $q^m_{2,n}$ are spherical harmonic coefficients of the potential vorticity q.

The spectral equations for enstrophy are obtained by following the procedure used for K.E. Spectral enstrophy equations in the zonal wave number m domain can be written in the form :

$$\frac{\partial (E_N)_m}{\partial t} = \frac{1}{4} \sum_{n=m}^{m+N} \left(q^m_{1,n} J^m_{1,n} + q^m_{2,n} J^m_{2,n} \right)$$

for $m \geq s$ 20(a)

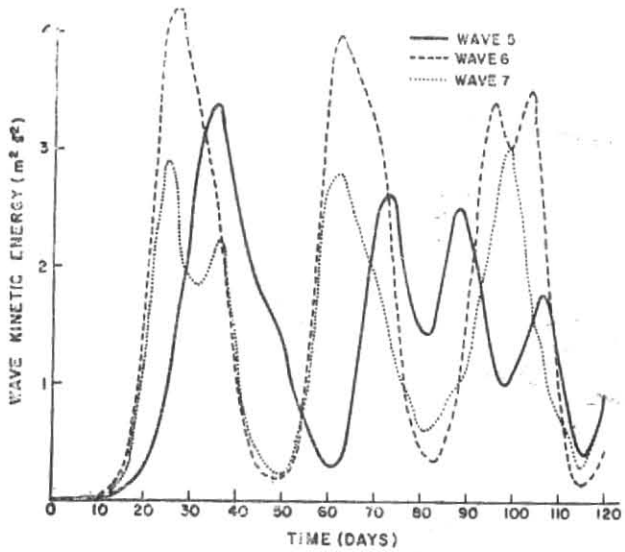

Fig. 1. Time variation of the global averaged wave kinetic energy per unit mass in $m^2\ s^{-2}$ for wave-zonal flow interaction experiment for waves 5, 6 and 7

$$\frac{\partial (E_N)_0}{\partial t} = \frac{1}{2} \sum_{n=1}^{N} q^0_{1,n}\ J^0_{1,n} \qquad 20(b)$$

The right hand side of Eqn. (20) denotes the transfer of enstrophy to wavenumber m from all other wavenumbers through the non-linear interactions. In order to isolate the wave-wave interaction process, the wave-zonal flow interaction, as given in Eqn. (3), is expressed in the spectral form :

$$C\,[(E_N)_0, (E_N)_m] = \frac{1}{4\pi a} \int_{-1}^{1} \sum_{n=0}^{N} q^0_{1,n}\ P^0_n \left(V_{1,m}\, q_{1,m} + V_{2,m}\, q_{2,m} \right) d\mu \qquad (21)$$

where $\frac{1}{2}(V_{1,m}\, q_{1,m} + V_{2,m}\, q_{2,m})$ is the zonal average potential vorticity flux at a latitude associated with wavenumber m. The spectral enstrophy equation in the two-dimensional wavenumber n domain is written in the form :

$$\frac{\partial}{\partial t} (E_N)_n = \frac{1}{2} (q^0_{1,n}\ J^0_{1,n}) + \frac{1}{4} \sum_{m=s}^{n} \left(q^m_{1,n}\ J^m_{1,n} + q^m_{2,n}\ J^m_{2,n} \right) \qquad (22)$$

3. Basic zonal flow

The meridional profile of zonal wind is obtained by averaging mean monsoon (June-August) zonal wind at 100 mb over the longitudinal belt : 55° E-105°E. The profile is fitted by a truncated Legendre series at $N = 20$. The same profile designated as F has been utilised in M 87 for investigating the influence of mid-latitude westerly jets on the linear unstable modes of the easterly jet. It may be noted that whereas the easterly jet satisfies the necessary condition for the barotropic instability, while the westerly jets do not satisfy the necessary condition.

4. Results

(a) *Single wave-zonal flow interaction*

In single wave-zonal flow interaction (quasi-linear) experiments, it is assumed that only one zonal wave is present throughout the integration. The initial single zonal wave m which corresponds to the most unstable linear mode is considered. The initial perturbation is normalised by specifying its global area averaged kinetic energy as 10^{-4} of the global averaged kinetic energy of the basic zonal current. This value for the normalisation is chosen based on the results of sensitivity of the wave-zonal interaction on the initial perturbation kinetic energy. It was found that the evolution of a single wave under wave-zonal flow interaction was rather insensitive to the further reduction to the global average initial wave kinetic energy of $1.3 \times 10^{-2}\ m^2\ s^{-2}$. For quasi-linear integration the rhomboidal truncation at $N=20$ is chosen and the model is integrated for 120 days. The zonal wave experiment is performed for the wavenumbers 5-7.

The time variation of the global area averaged wave kinetic energy per unit mass for wavenumbers 5-7 is shown in Fig. 1. It is clearly seen that the wave kinetic energy exhibits an oscillation with a period around 35 days. The time series of kinetic energy for waves 5-7 between day 16 and day 120 at the interval of one day was subjected to a power spectral analysis. The results indicated that the kinetic energy oscillation has a period of 35 days. The amplitude of oscillation for wave 6 is larger than that of waves 5 and 7.

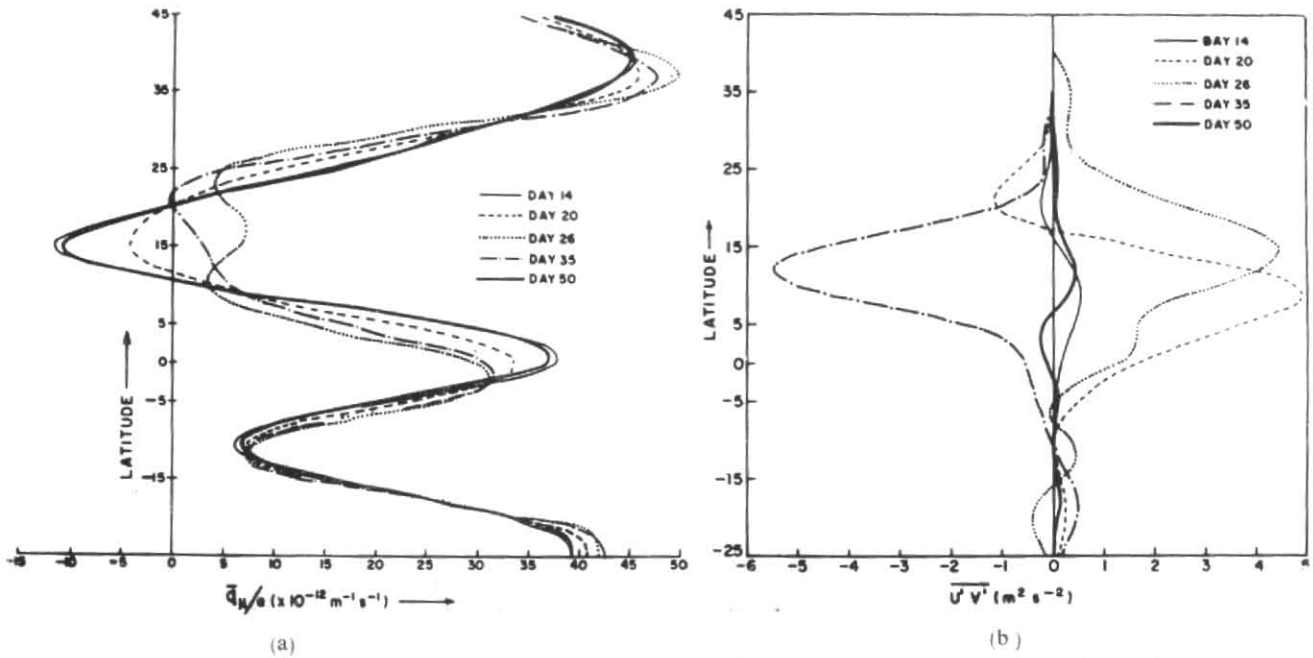

Fig. 2. (a) Meridional gradient of basic state potential vorticity $\bar{q}_\mu/a$ (10^{-12} m^{-1} s^{-1}) and (b) zonal angular momentum transport $\overline{U'V'}$ (m^2 s^{-2}) profiles for wavenumber 6 at various times in the wave-zonal flow interaction experiment

Frederiksen (1981) has also found the vacillation cycle in the non-linear integration of a multi-level primitive equation spectral model for the cases of initial single zonal waves 7 and 10, superposed on mean southern hemisphere zonal flow for January. Further, he concluded from a comparison between his results and those obtained by Simmons and Hoskins (1978), wherein they had not found vacillation cycle in their non-linear, experiments, that the existence of vacillation cycle is highly dependent on the nature of basic state. In a recent study Kwon and Mak (1988) have found the presence of vacillation cycle in a forced dissipative non-linear barotropic system when the forcing is sufficiently large.

An inspection of time variation of wave kinetic energy for wave 6 reveals that the wave commences its regular growth around day 14 after its initial adjustments. Thereafter, the wave kinetic energy increases exponentially till at around day 22. The wave attains the maximum growth rate at day 20. During the exponential increase of the wave kinetic energy the wave behaves as a linear wave and attains the growth rate which is almost equal to the linear maximum growth rate value. Beyond day 22 the increase in wave kinetic energy is slowed down considerably and it ceases to increase on day 26, when the energy attains its maximum value. The decrease in the energy is seen up to day 50. The computations of the barotropic energy conversion indicated that the wave received kinetic energy from the basic state during its growth phase while during its decay phase it loses the kinetic energy to the basic state.

It may be noted that after completion of the initial exponential growth phase at no other time during the integration the wave attains a growth rate comparable to its values during the exponential growth phase. Hence, we may conclude that at no time during the life cycle of growth and decay of disturbances, except for their initial formation, the non-linear interactions, particularly wave-zonal interaction, can be neglected.

The exponential amplification of the wave is arrested due to the modification of zonal flow as a result of wave-zonal interaction. The wave is no longer the most unstable mode for the modified zonal flow. It is quite possible that the structure of wave deviates considerably from the unstable modes. The angular momentum transport associated with the wave 6 and $\bar{q}\mu/a$ profiles for day 14, 20, 26, 35 and 50 are plotted and presented in Figs. 2(a) and 2(b) respectively.

As the wave grows exponentially after initial adjustments, it transports westerly angular momentum into the easterly jet centre (Fig. 2 a) and the transports are down the gradient of basic zonal flow. This process leads to increase in $\bar{q}\mu$ in the region where it is negative (Fig. 2b). $\bar{q}\mu>0$ throughout the domain at day 26 when the wave growth is stopped. Even though the necessary condition for the instability is not satisfied before day 26 itself the wave is seen to grow slowly but not exponentially. It may be noted in this connection that the necessary condition for instability is derived for the normal modes having exponential growth. During the decay phase of wave (day 26-day 50), the westerly angular momentum is transported away from the easterly jet centre. The negative region of $\bar{q}\mu$ is developed beyond day 35. Thus the necessary condition for the instability is satisfied beyond day 35, still the wave continues to decay.

$\overline{V'q'}$ & $(\overline{V'q'})_{\mu/a}$ profiles at different days are computed (not presented). A comparison of these profiles with corresponding $\bar{q}\mu/a$ profile (Fig. 2b) has indicated that during the wave growth convergence of the wave

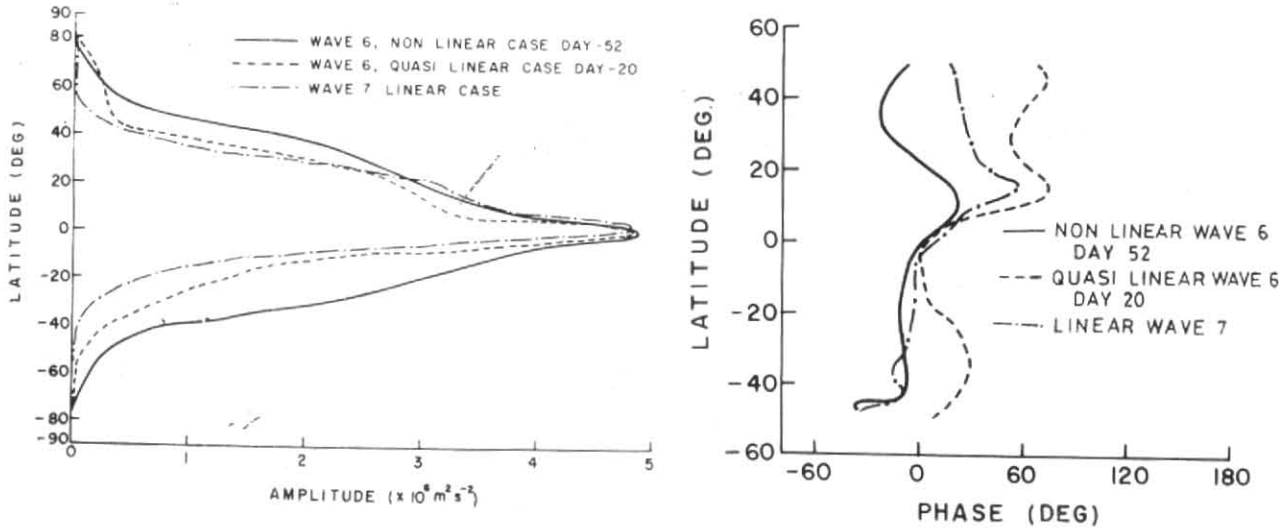

(a) (b)

Fig. 3. Meridional profiles of (a) stream function wave amplitude (10^6 m^2 s^{-1}) and (b) phase (deg) for linear wave 7, quasi-linear and non-linear wave 6

potential vorticity occurs in the negative region of $\bar{q}\mu/a$ so that the negative region is filled up while divergence of the wave potential vorticity takes place in the same region during the wave decay. Further, the wave potential vorticity flux is down the gradient of $\bar{q}$ during the wave growth and up the gradient during its decay.

To identify the importance of wave-zonal flow interaction in the development of waves, amplitude and phase profiles for the most unstable linear wave 7 and the exponentially growing wave 6 at day 20 of quasi-linear case are presented in Figs. 3 (a) and 3 (b) respectively. It is seen that the meridional phase tilt is larger for quasi-linear wave than for linear wave. Similarly, the meridional characteristic scale is larger for quasi-linear wave than for linear wave.

(b) *Wave-wave interaction experiment*

The initial state in the non-linear experiment is identical to the single wave-zonal flow interaction experiment. However, the first harmonic is generated due to the self interaction of the initial dominant wave and subsequent harmonics are generated due to self-interaction and interaction between different harmonics. The initial wave kinetic enegry is equal to the value used in the wave-zonal flow interaction experiments. The model is integrated for 120 days.

The global averaged wave kinetic energy per unit mass and enstrophy as a function of time are studied The time variations in two parameters are identical. The time vatiation of the wave kinetic engergy alone is presented in Fig. 5. A comparison between Figs. 1 and 5 reveals that the small amplitude high frequency oscillations are developed due to wave-wave interaction. Further, the wave-wave interaction leads to variation in the period of low frequency oscillations, which varies between 25&35 days, while in the case of wave-zonal interaction experiment the period of oscillation is fixed at 35 days. A further comparison between Figs. 1 and 5 indicates that wave-wave interactions do not allow the basic zonal flow to deviate from the neutral state as much as observed in wave-zonal flow interaction experiment.

Numerical experiments were performed in order to identify the effects of Rayleigh type of friction in the wave equation and the effect of a mechanism which tries to restore the vorticity to its initial value in the zonal vorticity equation. The details of the results from these experiments are not presented. The following conclusion was arrived at on the basis of the results. The low frequency oscillation is suppressed by the friction and is amplified by the restoring mechanism.

The meridional scale for exponentially growing wave in the non-linear case is larger than that for

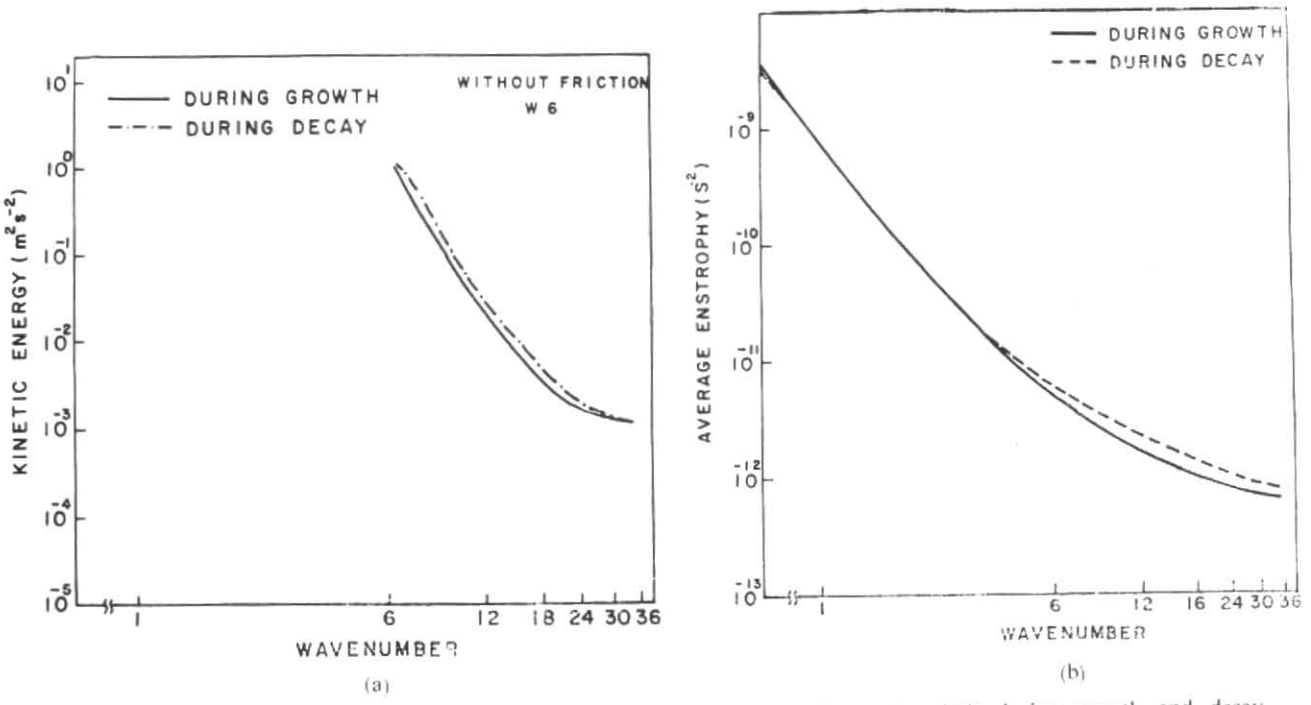

Fig. 4. Time mean and global average (a) kinetic energy ($m^2 s^{-2}$), (b) enstrophy spectra (s^{-2}) during growth and decay phases for wave-wave interaction experiment for the initial wave 6

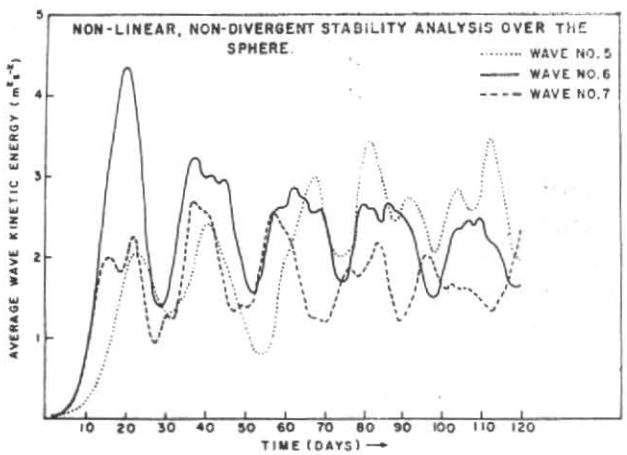

Fig. 5. Time variation of the global averaged wave kinetic energy per unit mass in $m^2 s^{-2}$ for wave-wave interaction experiment and for initial waves 5, 6 and 7

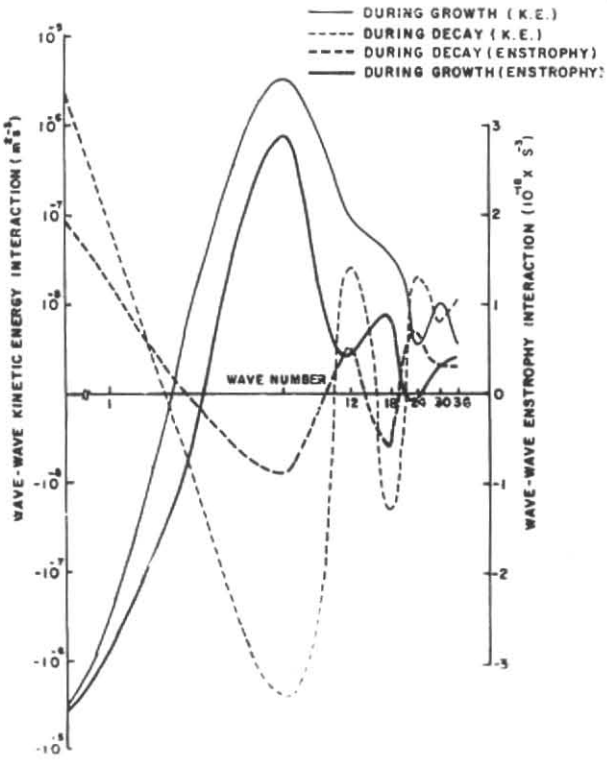

Fig. 6. Wave-wave interaction for kinetic energy ($m^2 s^{-3}$) and enstrophy ($10^{-18} s^{-3}$) as a function of zonal wavenumber m

quasi-linear and linear cases (Fig. 3a). The phase tilt is smaller than that of quasi-linear and linear cases (Fig. 3b).

The stream function distributions in λ-ϕ plane at the interval of 4 days were computed for the initial wave 6 case (not presented). An asymmetry in the zonal direction in the intensity of low and high is noticed. This asymmetry is due to the generation of additional waves as a consequence of non-linear interaction. A closed high around the latitude 35° N is seen in the stream function field obtained after superposition of perturbation field on the basic state. The intensity of high fluctuates with time.

Figs. 4 (a) and (b) show the time mean global average kinetic energy and enstrophy as a function of zonal wavenumber m. It is seen that the shape of energy and enstrophy spectra for the growth and decay phases are nearly the same. The kinetic energy and enstrophy during the decay phase are larger than that during growing phase for $m \leqslant 6$. This may be due to the relative slow decrease of kinetic energy from its state of maxima compared to the rise of kinetic energy towards the maxima. The kinetic energy spectra have approximate $m^{-5/3}$ power law for $6 \leqslant m \leqslant 24$ which is typical of inertial range power laws of two-dimensional turbulence. In the wavenumber range $m>24$, the power law followed by kinetic energy spectra is $m^{-1/2}$, which is near to the m^{-1} power law for inviscid two-dimensional turbulence (Fredriksen and Sowford 1980). The slow decrease in the kinetic energy spectra for the larger m is due to the accumulation of the energy in the largest wavenumber in the absence of dissipation. It is seen that the enstrophy spectra vary as m^{-2} in the wave number range $6 \leqslant m \leqslant 12$ and their variation is m in the range $18 \leqslant m \leqslant 36$. It was also noticed that the decrease in kinetic energy and enstrophy with $m^{-2/3}$ is rather sharp in the presence of dissipation and particularly for the larger m.

The dominant wave 6 receives the maximum kinetic energy from wave-zonal flow and wave-wave interactions during the growth of perturbation (Fig. 6). The wave-zonal flow and wave-wave interactions are rather weak for $m \geqslant 12$. The rate of loss of kinetic energy by the zonal flow (m=0) due to zonal wave interaction is little more than the rate of gain of energy by wave 6. This indicates that wave-zonal flow interaction is much stronger than the wave-wave interaction. All waves are receiving kinetic energy during the growing phase. During the decay phase, the maximum transfer of kinetic energy to the zonal flow takes place at wave 6, *via* wave-zonal flow interaction, while all other waves except wave 18 continue to receive the kinetic energy due to wave-wave interaction. It may also be noted that the rate of increase of kinetic energy of zonal flow is more than the rate of loss by wave 6; this implies that a part of energy received by the zonal flow from wave 6 is transferred to other growing waves *via* wave-zonal flow interaction.

5. Conclusion

It was intended to study the role of wave-zonal flow and wave-wave interactions in the non-linear dynamics of initial single growing barotropic wave over the sphere. For this purpose the evolution of perturbation superimposed on the unstable mean monsoon upper tropospheric tropical easterly jet at 100 mb was simulated by utilising the non-divergent barotropic global spectral model. It was found that the wave-zonal flow interaction dominates over the wave-wave interaction. Further, the non-linear wave is more realistic than the linear wave. Some of the asymmetries in the disturbance can be attributed to the wave-wave interactions.

It was not possible to explain satisfactorily the growth of waves even though the necessary condition for barotropic instability is not satisfied by the zonal flow.

Acknowledgements

The author is thankful to Smt. S.S. Desai and Shri D. W. Ganer for their help in preparation of the manuscript. He wishes to thank Smt. S.S. Naik for typing the manuscript.

References

Frederiksen, J.S., 1981, Growth and vacillation cycles of disturbances in Southern Hemisphere Flows, *J. atmos. Sci.*, **38**, 673-689.

Frederiksen, J.S. and Sowford, B.L., 1980, Statistical dynamics of two dimensional inviscid flow on a sphere, *J. atmos. Sci.*, **37**, 717-732.

Kwon, J.H. and Mak, M., 1988, On the equilibration in non-linear barotropic instability, *J. atmos. Sci.*, **45**, 294-308.

Mishra, S.K., Subrahmanyam, D. and Tandon, M.K., 1981, Divergent barotropic instability of the tropical asymmetric easterly jet, *J. atmos. Sci.*, **38**, 2164-2171.

Mishra, S.K. and Tandon, M.K., 1983, A combined barotropic-baroclinic instability study of the upper tropospheric tropcal easterly jet, *J. atmos. Sci.*, **40**, 2708-2723.

Mishra, S.K., 1987, Linear barotropic instability of the tropical easterly jet on a sphere, *J. atmos. Sci.*, **44**, 373-383.

Schoeberl, M.R. and Lindzen, R.S., 1984, A numerical simulation of barotropic instability : Part I—Wave mean flow interaction, *J. atmos. Sci.*, **41**, 1368-1379.

Simmons, A.J. and Hoskins, B.J., 1978, The life cycles of some non-linear baroclinic waves, *J. atmos. Sci.*, **35**, 414-432.

Tupaz, J.B., Williams, R.T. and Chang, C.P., 1978, A numerical study of barotropic instability in a zonally varying easterly jet, *J. atmos. Sci.*, **35**, 1265-1280.

Williams, R.T., Lin, H. and Chang, C.P., 1984, Non-linear and linear effects in an easterly jet with downstream variation, *J. atmos. Sci.*, **41**, 621-626.